THz Letters

Terahertz Sieves

Federico Machado, Przemysław Zagrajek, Juan A. Monsoriu, and Walter D. Furlan

***Abstract*—Imaging at terahertz (THz) frequencies offers a great potential for applications including security screening, telecommunications biodetection, and spectroscopy. Some of these applications need specially designed lenses with customized characteristics that are not commercially available. In this letter, we present the THz sieves as a new kind of THz lenses. We demonstrate that these lenses improve the resolution of conventional zone plates constructed with the same level of detail. Amplitude and phase THz sieves were three-dimensional printed and tested experimentally. Excellent agreement was obtained between the experimental and calculated results.**

***Index Terms*—Imaging, photon sieves (PSs), terahertz (THz) focusing, THz materials.**

I. Introduction

NUMEROUS applications of terahertz (THz) a sub-THz radiation such as imaging or spectroscopy require passive devices such as lenses [1], filters [2], and waveguides [3]. Focusing lenses allow improving the sensitivity of THz setups, which is a crucial issue in this range of electromagnetic radiation, where there is a lack of high-power sources and high-sensitive detectors.

The optical properties of different polymers [4] have been exploited to fabricate a variety of THz lenses that are commercially available. However, many applications require custom-made THz lenses with special designs. Refractive lenses with different geometries have been manufactured from bulk polymers by lathe turning, compression molding [1], and recently, by three-dimensional (3-D) printing [5], [6]. On the other hand, diffractive THz optical elements have been proposed and tested [7], [8]. In spite of their lower light throughput and chromatic aberration, diffractive lenses can have high numerical aperture [9] and permit beam shaping [10], [11], working in linear and compact setups. Therefore, in many applications, the performance of diffractive THz lenses is better than that of their refractive homologous. Additionally, 3-D printing technology has also been used recently to construct special designs of diffractive lenses [10]–[12]. As different materials used for 3-D printing have low refractive index and a frequency-dependent absorbance in the THz bandwidth, several 3-D printing materials were tested previously in our previous paper [10]. In particular, using THz time-domain spectroscopy we measured the absorption coefficients and refractive index of nylon polyamide (PA6) and acrylonitrile-butadiene-styrene with different densities in the 0.1–2.0 THz frequency range.

Photon sieves (PSs) are diffractive optical elements, originally conceived to improve X-rays focusing [13]. The first PSs were basically amplitude Fresnel zone plates (FZPs) in which the transparent rings were substituted by nonoverlapping holes of different sizes. Special features of PSs in the visible range were investigated in several works [14]–[17], from which different applications emerged [18], [19]. The main features that characterize PSs are the following.

1) They can be fabricated on a single sheet without any substrate.
2) Despite its lower efficiency, a PS allows better resolution than an FZP, with the same dimensions [13].
3) PSs allow improved focusing by the suppression of secondary maxima and higher orders of diffraction [16], [17].

In this letter, we introduce the THz sieves (TSs). We study the TS axial and transverse resolution in comparison with those provided by a conventional FZP constructed with the same level of detail. The focusing properties of both amplitude and phase TSs are experimentally demonstrated.

II. TSs. Design and Focusing Properties

The construction procedure of a TS starts from a conventional FZP designed for a given THz frequency. As it is well known, an amplitude FZP of focal length f at wavelength λ, consists of alternate transparent and opaque zones, where the radius of the nth zone is given by $r_n^2 = 2nf\lambda + n^2\lambda^2$. The width of outermost ring of a zone plate with N zones, $w = r_N - r_{N-1}$ [see Fig. 1(a)], imposes a limit on the maximum resolution achievable with the FZP: $w = \lambda f / 2r_N$. It was shown in [13] that a PS

Manuscript received August 10, 2017; accepted September 30, 2017. Date of publication November 1, 2017; date of current version January 9, 2018. This work was supported in part by the Ministerio de Economía y Competitividad and FEDER, Spain, under Grant DPI2015-71256-R, in part by the Generalitat Valenciana under Grant PROMETEOII-2014-072, Spain, and in part by the National Center for Research and Development in Poland under Grant LIDER/020/319/L-5/13/NCBR/2014. *(Corresponding author: Juan A. Monsoriu.)*

F. Machado and J. A. Monsoriu are with the Centro de Tecnologías Físicas, Universitat Politècnica de València, Valencia 46020, Spain (e-mail: femacol@doctor.upv.es; jmonsori@fis.upv.es).

P. Zagrajek is with the Institute of Optoelectronics, Military University of Technology, Warsaw 01-476, Poland (e-mail: przemyslaw.zagrajek@wat.edu.pl).

W. D. Furlan is with the Departamento de Óptica y Optometría y Ciencias de la Visión, Universitat de València, Burjassot E-46100, Spain (e-mail: walter.furlan@uv.es).

Color versions of one or more of the figures in this letter are available online at http://ieeexplore.ieee.org.

Digital Object Identifier 10.1109/TTHZ.2017.2762292

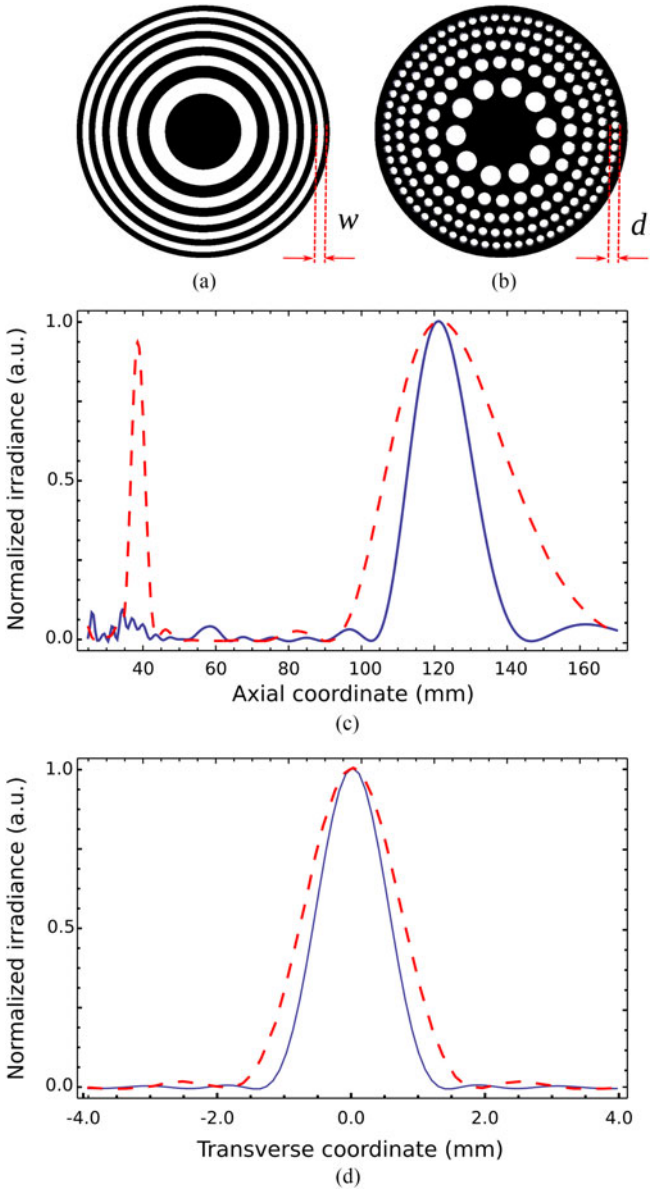

Fig. 1. (a) Binary FZP, w is the width of the outermost zone, which determines its transverse resolution. (b) THz sieve with the same number of Fresnel zones, d is the diameter of the holes at the Fresnel zone corresponding to w. (c) Numerical axial PSF and (d) transverse intensity at the focal plane, computed for a FZP (dashed line) and a TS (continuous line) of the same focal distance ($f = 122$ mm; $\nu_0 = 0.625$ THz). In (c) and (d), each plot was normalized to its maximum value.

can overcome this limitation because the pinhole diameter can be bigger than the width of the underlying zone. Thus, a PS can have a higher numerical aperture than an FZP constructed with the same level of detail. This property is of particular interest in THz applications, where low-cost diffractive lenses can be 3-D printed.

A TS is constructed by replacing the transparent rings of width w in the FZP by nonoverlapping circular holes of diameter d distributed about the rings [see Fig. 1(b)]. Thus, the transmittance function $t(x, y)$ of a TS can be expressed as a binary function that takes the values $t(x, y) = 1$ if $(x - x_i)^2 + (y - y_i)^2 \leq (d_i/2)^2$; and either $t(x, y) = 0$ or $t(x, y) = -1$, otherwise; depending on if the TS is of amplitude or phase, respectively. In the transmittance function, x_i and y_i are the center coordinates of the ith hole.

The focusing properties of our proposal were assessed in comparison with an FZP by means of the irradiance at different planes for a point object at infinity, i.e., the point spread function (PSF). This function was computed numerically by using the nonparaxial scalar diffraction theory

$$I(x, y; z) = 1/\lambda^2 \times \left| \iint t(x_0, y_0) \frac{\exp\left\{i \frac{2\pi}{\lambda} \sqrt{(x-x_0)^2+(y-y_0)^2+z^2}\right\}}{\sqrt{(x-x_0)^2+(y-y_0)^2+z^2}} dx_0\, dy_0 \right|^2. \quad (1)$$

We employed (1) to compare the focusing properties of phase TS and FZP. In particular, we analyzed two lenses of the same focal distance: $f = 122$ mm, at the same design frequency: $\nu_0 = 0.625$ THz. For the lens material, we considered polyamide PA6, which has a refractive index $n = 1.59$ at this frequency [10]. The radius of the FZP ($r_N = 18.8$ mm) and its outermost width ($w = 1.63$ mm), were both selected to be compatible with an experimental verification in our laboratory. The numerical aperture of the FZP was NA $= 0.154$. For the TS, the minimum hole diameter was fixed to be $d_{\min} = 1.65$ mm; i.e., approximately of the same size of w. The maximum hole diameter was $d_{\max} = 4.11$ mm. The hole density in each zone was chosen so that the transparent area in each TS zone will be at least a 75% of the whole Fresnel zone. With these parameters we used (1) to compute the axial irradiance provided by the TS for different values of d, in the range $1w \leq d \leq 2w$, obtaining the value $d = 1.33w$ provided the best apodization of the third diffraction order focus. Thus, we found that with the same width of the outermost ring, the numerical aperture of the TS was NA $= 0.2$, i.e., 1.33 times higher than the FZP, being the TS radius $r_N = 25$ mm.

The axial irradiances and transverse intensities at the focal plane, provided by both lenses are shown in Fig. 1(c) and (d), respectively. As can be seen in Fig. 1(c) and (d), both the axial and transverse resolutions are better for the TS. The full width at half-maximum (FWHM) of the axial irradiance peak provided by the TS is 18.8 mm, which is 52% lower than FWHM of the FZP. For the transverse resolution, the FWHM at the focus of the TS is 1.31 mm and 1.77 for the FZP. The apodization of the third-order focus at $z = 40$ mm can be clearly seen in Fig. 1(c). The physical reason for this apodization is that the axial irradiance depends only on the angular average of the effective pupil along the radial coordinate [20], which in the case of TS is smoothed by effect of the holes. On the other hand, as expected [13], we also found that the diffraction efficiency of the FZP was higher (40.5%) than the diffraction efficiency of the TS (18.4%).

In order to investigate the effect of a finite bandwidth on TS performance, we have computed the axial PSF for the TS at two other frequencies. The result is shown in Fig. 2. In this case in addition to the focal shift produced by the chromatic

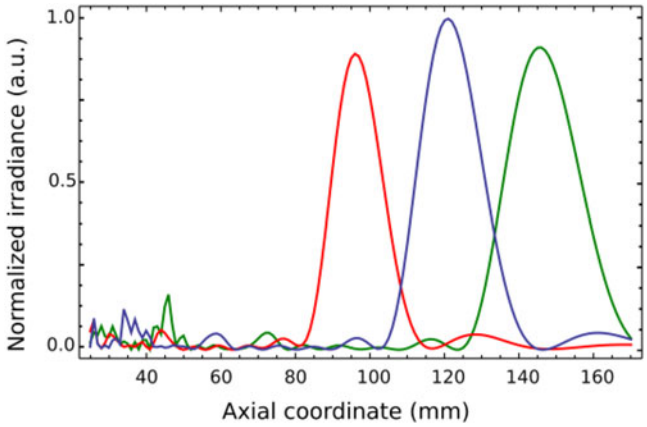

Fig. 2. TS performance at three different frequencies: $\nu_0 = 0.625$ THz (blue line); $\nu_1 = 0.500$ THz (red line) and $\nu_2 = 0.750$ THz (green line). The maximum value of the irradiance for the design frequency was used for normalization.

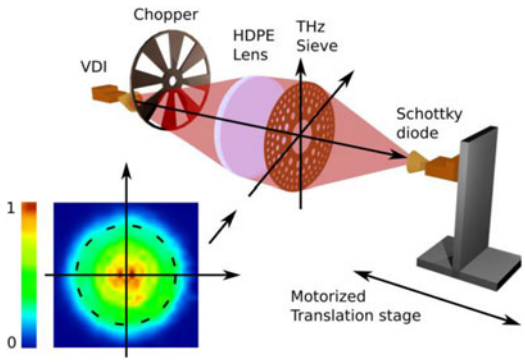

Fig. 3. Experimental setup used in axial PSF measurements. The source of THz is a VDI frequency multiplier with a horn antenna. The divergent beam, is collimated by a HDPE refractive lens (focal distance $f = 150$ mm). The transverse intensity measured at TS plane (x, y) is shown in the inset. The radius of the dashed line in the inset is $r_N = 18.8$ mm. The detector: A Schottky diode, with a horn antenna, mounted on a 3-D motorized stage, scanned the focal volume. A lock-in system, based on modulation at 187 Hz, and a mechanical chopper, was employed to measure the signal from the detector.

aberration of the TS, the peak intensity is lower for the other two frequencies because for these frequencies the phase difference between the holes and the plate is not exactly π.

III. Experimental Results

Fig. 3 shows the setup we employed for the experimental characterization of the TSs. A VDI frequency multiplier (Virginia Diodes, Inc., Charlottesville, VA, USA) provided the 0.625 THz beam. The source of microwave radiation for the VDI frequency multiplier was an electromagnetic YIG-tuned oscillator MLXB-1768PA. It generates radiation in frequency range 13–15 GHz. The base frequency was multiplied 48 times. The divergent beam, emerging from the horn antenna, was collimated by a high-density polyethylene (HDPE) lens and directed to the investigated TS. The detector, a Schottky diode, was mounted on a 3-D motorized stage. The focal spot was scanned with a horn antenna, having a 2.4-mm-aperture diameter. A lock-in system, based on modulation at 187 Hz, and a mechanical chopper, was employed to measure the signal from the detector. The inset in

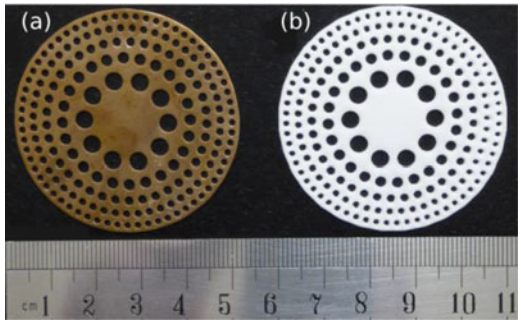

Fig. 4. 3-D printed TSs. (a) Is an amplitude lens made in bronze. (b) Is a phase lens made in PA6 polyamide. The holes are located in the even zones of an FZP (focal distance $f = 122$ m.

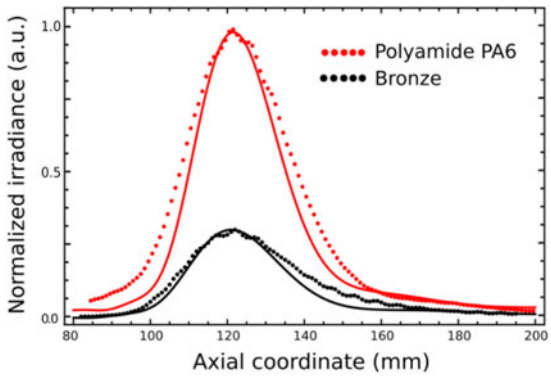

Fig. 5. Axial irradiances provided by the 3-D printed THz lenses shown in Fig. 4. Experimental data are represented with dotted lines; and the corresponding numerical simulations by continuous lines. The maximum value of the irradiance for the PA6 lens was used for normalization.

Fig. 3 shows the intensity recorded at the transverse plane (x, y) just before the lens plane.

Two different TS lenses were fabricated by 3-D printing: An amplitude lens, shown in Fig. 4(a), constructed in bronze, and a phase lens, shown in Fig 4(b), made in PA 6 polyamide (refractive index 1.59 and absorption coefficient 3.09 cm^{-1} at 0.625 THz). The physical dimensions of both lenses were the same and coincide with those used to compute [see Fig. 1(c) and (d)]. As the minimum thickness of the phase TS that provides a π phase difference between the lenses material and the holes $t = \lambda/2(n-1) = 0.4$ mm was considered too thin to be handled, we have constructed the lenses with a thickness of $3t = 1,2$ mm, which produces the same phase shift. Other details of the 3-D lens production can be found elsewhere [10].

Fig. 5 shows the experimental results obtained for the axial PSF (dotted lines) corresponding to the lenses shown in Fig. 4. The numerical simulations obtained with (1) are shown in the same figure for comparison (continuous lines). To obtain the numerical results, the transmittance of the lens was multiplied by the normalized field amplitude recorded at the lens plane (x, y) shown in Fig. 3. In addition, instead of a point-like detector as in Fig. 1(c), we integrated the irradiance over the detection area of the horn antenna. Note that, in spite of that the surface roughness and microstructure of the 3-D printed lenses have not been considered, we found a very good agreement between

theory and experiment. As expected phase polyamide TS is four times more efficient than the amplitude bronze TS of the same dimensions.

IV. Conclusion

By using 3-D printing technology, we have demonstrated the feasibility of realizing TS diffractive lenses. The focusing properties of both: Amplitude and phase TS were tested using a 0.625 THz beam. We have shown that TS can achieve better resolution than binary FZP. Further improvements are expected with other exotic sieves distributions [15], [16]. So, our proposal opens the possibility to use low-cost optics for a wide range of THz applications. Two examples of special interest are THz astronomical telescopes where ultralarge space telescope primaries are necessary, preferably as a single membrane, i.e, with no supporting structure [19], [21] and THz compressive sensing, to achieve the precise focalization needed in a single pixel camera [22].

References

[1] B. Scherger, M. Scheller, C. Jansen, M. Koch, and K. Wiesauer, "Terahertz lenses made by compression molding of micropowders," *Appl. Opt.*, vol. 50, no. 15, pp. 2256–2262, May 2011.

[2] R. Wilk, N. Vieweg, O. Kopschinski, and M. Koch, "Liquid crystal based electrically switchable Bragg structure for THz waves," *Opt. Express*, vol. 17, no. 9, pp. 7377–7382, Apr. 2009.

[3] M. D'Auria *et al.*, "3-D printed metal-pipe rectangular waveguides," *IEEE Trans. Compon. Packag. Manuf. Technol.*, vol. 5, no. 9, pp. 1339–1349, Sep. 2015.

[4] A. Podzorov and G. Gallot, "Low-loss polymers for terahertz applications," *Appl. Opt.*, vol. 47, no. 18, pp. 3254–3257, Jun. 2008.

[5] S. F. Busch, M. Weidenbach, M. Fey, F. Schäfer, T. Probst, and M. Koch, "Optical properties of 3D printable plastics in the THz regime and their application for 3D printed THz optics," *J. Infrared Millim. THz Waves*, vol. 35, no. 12, pp. 993–997, Dec. 2014.

[6] A. D. Squires, E. Constable, and A. Lewis, "3D printed terahertz diffraction gratings and lenses," *J. Infrared Millim. THz Waves*, vol. 36, no. 1, pp. 72–80, Jan. 2015.

[7] S. Wang *et al.*, "Characterization of T-ray binary lenses," *Opt. Lett.*, vol. 27, no. 13, pp. 1183–1185, Jul. 2002.

[8] Y. Yu and W. Dou, "Generation of pseudo-Bessel beams at THz frequencies by use of binary axicons," *Opt. Express*, vol. 17, no. 2, pp. 888–893, Jan. 2009.

[9] A. Siemion *et al.*, "Diffractive paper lens for terahertz optics," *Opt. Lett.*, vol. 37, no. 20, pp. 4320–4322, Oct. 2012.

[10] W. D. Furlan, V. Ferrando, J. A. Monsoriu, P. Zagrajek, E. Czerwińska, and M. Szustakowski, "3D printed diffractive terahertz lenses," *Opt. Lett.*, vol. 41, no. 8, pp. 1748–1751, Apr. 2016.

[11] C. Liu, L. Niu, K. Wang, and J. Liu, "3D-printed diffractive elements induced accelerating terahertz Airy beam," *Opt. Express*, vol. 24, no. 25, pp. 29342–29348, Dec. 2016.

[12] J. Suszek *et al.*, "3-D-printed flat optics for THz linear scanners," *IEEE Trans. THz Sci. Technol.*, vol. 5, no. 2, pp. 314–316, Mar. 2015.

[13] L. Kipp *et al.*, "Sharper images by focusing soft x-rays with photon sieves," *Nature*, vol. 414, pp. 184–188, Nov. 2001.

[14] Q. Cao and J. Jahns, "Nonparaxial model for the focusing of high-numerical-aperture photon sieves," *J. Opt. Soc. Amer. A, Opt. Image Sci.*, vol. 20, no. 6, pp. 1005–1012, Jun. 2003.

[15] F. Giménez, J. A. Monsoriu, W. D. Furlan, and A. Pons, "Fractal photon sieve," *Opt. Express*, vol. 14, no. 25, pp. 11958–11963, Oct. 2006.

[16] F. Giménez, W. D. Furlan, and J. A. Monsoriu, "Lacunar fractal photon sieves," *Opt. Commun.*, vol. 277, no. 1, pp. 1–4, Sep. 2007.

[17] A. Sabatyan and S. Mirzaie, "Efficiency-enhanced photon sieve using Gaussian/overlapping distribution of pinholes," *Appl. Opt.*, vol. 50, no. 11, pp. 1517–1522, Apr. 2011.

[18] R. Menon, D. Gil, G. Barbastathis, and H. Smith, "Photon-sieve lithography," *J. Opt. Soc. Amer. A, Opt. Image Sci.*, vol. 22, no. 2, pp. 342–345, Feb. 2005.

[19] G. Andersen, "Large optical photon sieve," *Opt. Lett.*, vol. 30, no. 22, pp. 2976–2978, Nov. 2005.

[20] C. J. R. Sheppard and Z. S. Hegedus, "Axial behavior of pupil-plane filters," *J. Opt. Soc. Amer. A, Opt. Image Sci.*, vol. 5, pp. 643–647, 1988.

[21] S. Withington, "Terahertz astronomical telescopes and instrumentation," *Philosoph. Trans. Roy. Soc. London A, Math, Phys. Sci.*, vol. 362, no. 1815, pp. 395–402, Feb. 2004.

[22] C. M. Watts *et al.*, "Terahertz compressive imaging with metamaterial spatial light modulators," *Nat. Photon.*, vol. 8, no. 8, pp. 605–609, Jun. 2014.